

# DGSUnet: An Improved Unet Model with DINO-Guided SAM2 for Multi-Scale Feature Collaboration

Yimin Xu<sup>1,2</sup>

<sup>1</sup> Chengdu Institute of Computer Application, Chinese Academy of Sciences, Chengdu Sichuan 610213, China

<sup>2</sup> University of Chinese Academy of Sciences, Beijing 100049, China  
xuyimin23@mails.ucas.ac.cn

**Abstract.** Despite the significant advancements in general image segmentation achieved by large-scale pre-trained foundation models (such as Meta's Segment Anything Model (SAM) series and DINOv2), their performance in specialized fields remains limited by two critical issues: the excessive training costs due to large model parameters, and the insufficient ability to represent specific domain characteristics. This paper proposes a multi-scale feature collaboration framework guided by DINOv2 for SAM2, with core innovations in three aspects: (1) Establishing a feature collaboration mechanism between DINOv2 and SAM2 backbones, where high-dimensional semantic features extracted by the self-supervised model guide multi-scale feature fusion; (2) Designing lightweight adapter modules and cross-modal, cross-layer feature fusion units to inject cross-domain knowledge while freezing the base model parameters; (3) Constructing a U-shaped network structure based on U-net, which utilizes attention mechanisms to achieve adaptive aggregation decoding of multi-granularity features. This framework surpasses existing state-of-the-art methods in downstream tasks such as camouflage target detection and salient object detection, without requiring costly training processes. It provides a technical pathway for efficient deployment of visual image segmentation, demonstrating significant application value in a wide range of downstream tasks and specialized fields within image segmentation. Project page: <https://github.com/CheneyXuYiMin/SAM2DINO-Seg>

**Keywords:** SAM, DINO, Pre-training, Feature Fusion, U-Net.

## 1 Introduction

Image segmentation, as a core task in computer vision, aims to divide an image into regions with semantic meaning. Its core includes semantic segmentation (assigning category labels to each pixel) and instance segmentation (further distinguishing different instances within the same category). In recent years, with the breakthroughs in deep learning technology, image segmentation has played a crucial role in various natural domains such as medical image analysis (e.g., tumor boundary localization, organ segmentation) and autonomous driving (e.g., road scene understanding, obstacle

detection), becoming an important technical support for the practical application of artificial intelligence.

Meta's SAM [1] series and DINOv2 [2] visual foundation models, with their excellent model architecture design and extensive pre-training data, have achieved outstanding results in the field of general image segmentation, bringing potential for the development of downstream tasks in image segmentation. However, existing methods still face multiple challenges. Firstly, as foundational models, SAM2 and DINOv2 perform poorly in many subdomains such as salient object segmentation and camouflaged target segmentation without manual prompts. The main reasons are feature sparsity and the specificity of category samples, often leading to errors in foreground-background segmentation and results where the segmented regions are unrelated to the specified categories without human intervention. This phenomenon indicates that relying solely on foundational models is insufficient for downstream tasks like image segmentation in broad vertical domains. How to better apply these foundational models to specific categories and tasks in image segmentation, to achieve professionalism and adaptability in these application scenarios, holds significant research value.

To address the difficulties in image segmentation encountered in special downstream tasks based on large-scale pre-trained foundational models, this paper proposes DGSUnet, an improved Unet model based on DINO feature-guided SAM2 multi-scale feature collaboration. Its main features include:

- There is no need for full-parameter training of the pre-trained model, which requires fewer training resources, enabling the training of large models on resource-constrained devices.
- Simultaneously utilize DINOv2 and SAM2 as encoders, organically integrating the features extracted by both, leveraging the self-supervised training advantages of DINOv2 to compensate for the biases and hallucinations that occur during the feature extraction phase of the SAM model.
- Extensive experiments on multiple datasets demonstrate that DGSNet surpasses existing state-of-the-art methods in both accuracy and efficiency, establishing itself as a new benchmark in the field of image segmentation.

## 2 Related Work

### 2.1 U-Net Network and Its Improvements

U-Net [3] is an encoder-decoder architecture specifically designed for medical image segmentation, which addresses the segmentation challenges in small sample datasets by integrating multi-scale features through skip connections. Its upsampling path transmits contextual information across numerous feature channels, and when combined with a data augmentation strategy involving random elastic deformations, it significantly enhances the robustness of medical image segmentation. The original U-Net

excels in tasks such as cell segmentation, but its adaptability to complex scenarios (such as multi-scale targets and noise interference) remains limited. Building on this, researchers have proposed improved models. Zhou et al. [4] introduced multi-scale feature fusion into the U-Net, capturing features at different scales through multiple branches. Jha et al. [5] integrated residual modules, channel compression excitation mechanisms, and spatial pyramid pooling to achieve more efficient and precise semantic segmentation. With the rapid development of Transformer in natural language-related models, Chen et al. [6] combined the Transformer structure, which emphasizes global information, with CNNs that capture low-level image features for hybrid encoding, significantly enhancing the segmentation performance of U-Net. Cao et al. [7], aiming to address the continued reliance on CNN networks in TransUNet, proposed using Swin Transformer [8] as the backbone for the U-Net encoder, creating the first purely Transformer-based semantic segmentation model.

## 2.2 Segmentation Anything Model

The Segmentation Anything Model (SAM) is a revolutionary image segmentation model developed by Meta AI, whose core feature lies in its promptable universal segmentation capability. It can quickly identify and segment any object in an image through simple inputs such as clicks, bounding boxes, and text. From the release of SAM in 2023 to the release of SAM2 in 2024, it rapidly became a research hotspot in both academia and industry, regarded as a milestone in the field of computer vision. Research using SAM as a base model has achieved certain results in other vertical domains. Chen et al. [9] proposed adding an Adapter to the SAM model, enabling the model to adapt to downstream segmentation tasks in different fields. Yang et al. combined the SAM model with the U-Net architecture and trained it on a large dataset of medical segmentation images, achieving zero-shot medical image segmentation and obtaining a pre-trained model for general medical image segmentation. Xiong et al. [10] proposed using Hiera from SAM2 as the U-Net encoder, achieving SOTA performance in multiple downstream tasks.

## 2.3 DINO Model

DINO [2, 11] (Distillation and NO labels) is a self-supervised visual learning model proposed by Facebook AI in 2021. At its core, it is based on the Transformer architecture and achieves unsupervised feature learning through knowledge distillation. Consequently, compared to supervised learning, the features in DINO's latent space are sufficiently rich, enabling it to discern minute differences within objects, which holds significant importance for image segmentation tasks.

## 3 Method

The traditional U-Net model uses models like ResNet and ViT as visual feature extractors, which either lack the ability to extract multi-scale features or have a large number

of model parameters, making training difficult. The Hiera module in the SAM2 model not only has a hierarchical structure but also has been pre-trained on massive segmentation datasets, making it highly suitable for use as a feature extractor in the U-Net segmentation network. Experiments where SAM2 Hiera is used as the backbone to extract image features, as shown in Figure 1, reveal that the features extracted by Hiera perform well under low-dimensional PCA visualization but poorly in high dimensions. T-SNE visualization also indicates that feature-level clustering performs better in low dimensions and worse in high dimensions. Conversely, the ViT pre-trained network in the DINOv2 model, proposed based on a self-supervised mechanism, exhibits the opposite behavior when extracting features, as shown in Figure 2. Based on this discovery, a DINOv2 high-dimensional feature-guided SAM2 feature collaborative fusion model is proposed. The model architecture is depicted in Figure 3.

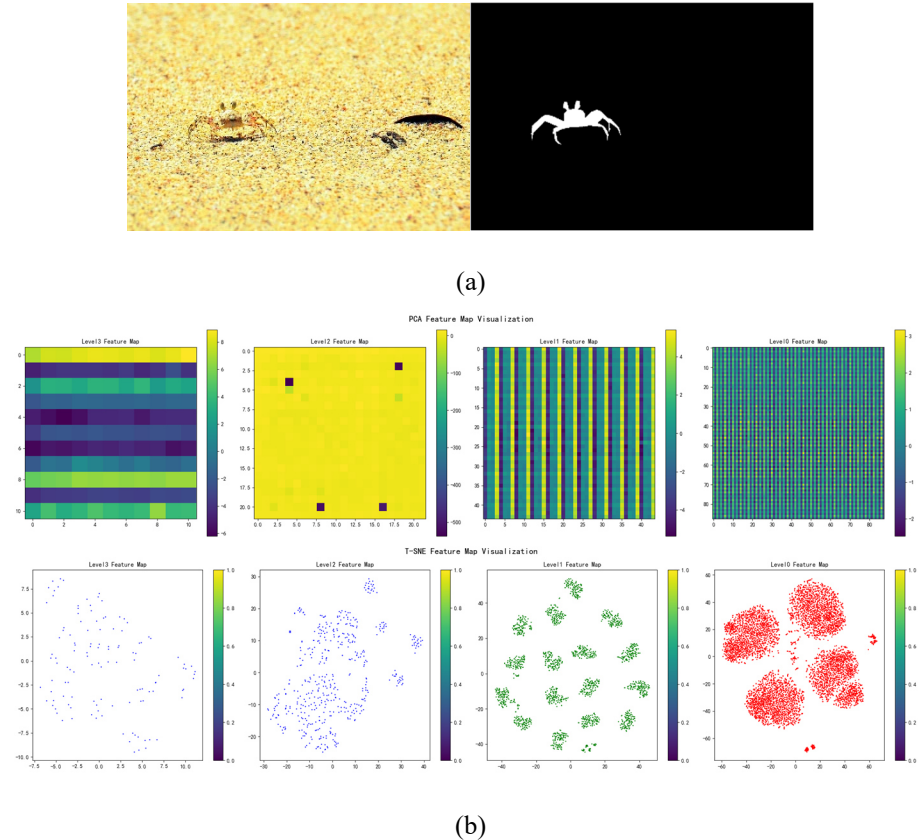


**Fig. 1.** (a) Input Image and Its Corresponding Ground Truth (b) Visualization of Features Extracted by SAM2 Hiera at Different Levels Using PCA and T-SNE Dimensionality Reduction.

DGSUnet utilizes the SAM2 Hiera module and DINOv2 ViT module as feature extraction components, incorporating multiple feature fusion modules and channel

transformation mechanisms. The overall design is based on the U-Net symmetric encoder-decoder architecture.

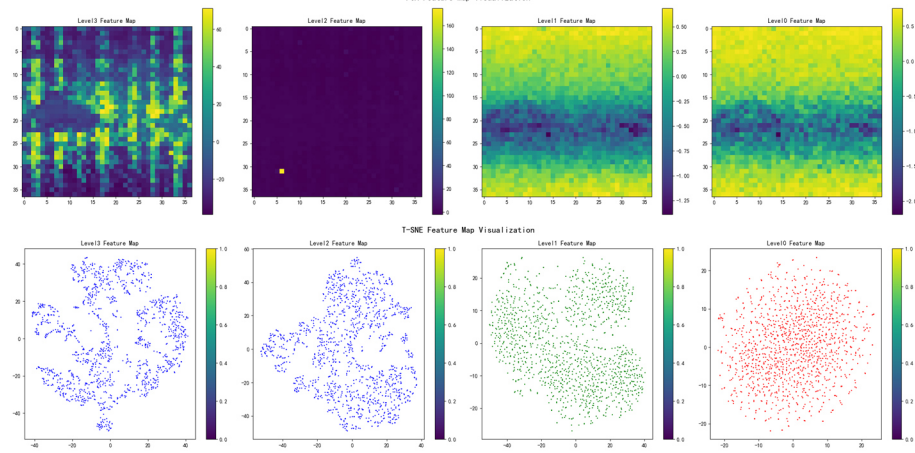


**Fig. 2.** DINOv2 ViT Feature Extraction at Different Levels with PCA and T-SNE Dimensionality Reduction Visualization.

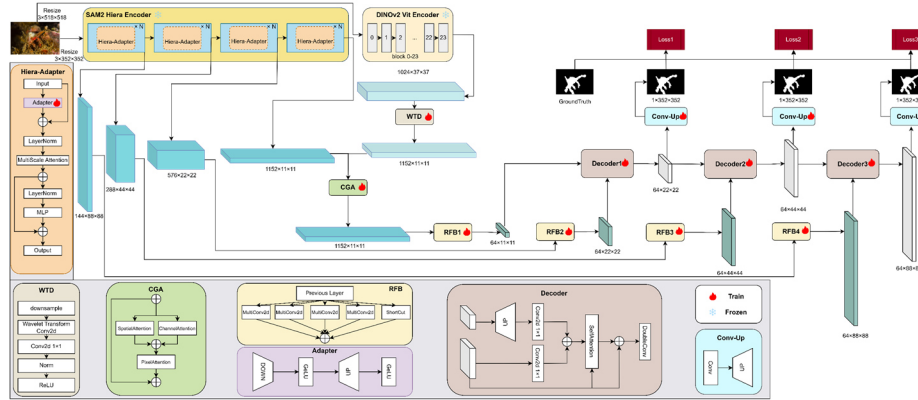


**Fig. 3.** DGSUnet Model Architecture Diagram.

**Encoder.** In DGSUnet, the Hiera module from SAM2 is used as the backbone of the feature extractor. The feature map output from the 24th layer Block of the ViT module in DINOv2 is injected as external knowledge into the last feature map extracted by Hiera, guiding the Hiera feature synergy from high-level semantic features to compensate for the loss of semantics and lack of detail in its high-level features. It is worth noting that this network freezes the pre-trained parameters of SAM2 Hiera and DINOv2 ViT, efficiently utilizing open-source models to reduce training costs. The input image is scaled to  $I \in \mathbb{R}^{3 \times 352 \times 352}$  before entering the Hiera module. After passing through the Hiera module, it outputs four feature maps at different levels, ranging from low to high as  $S_i \in \{\mathbb{R}^{144 \times 88 \times 88}, \mathbb{R}^{288 \times 44 \times 44}, \mathbb{R}^{576 \times 22 \times 22}, \mathbb{R}^{1152 \times 11 \times 11}\}$ . Before entering the DINOv2 ViT

module, it is scaled to  $I \in \mathbb{R}^{3 \times 518 \times 518}$ , and after passing through the last Block, the output feature map is  $V \in \mathbb{R}^{1024 \times 37 \times 37}$ . The Hiera and ViT used above are the pre-trained Hiera-L and ViT14, respectively.

**Adapter.** The Hiera module has an extremely large number of parameters, making the training time and physical costs prohibitively high. Additionally, considering the need to leverage the powerful feature extraction capabilities of pre-trained models, we introduced the Adapter module, referencing SAM-Adapter [9] and SAM2-Unet [10]. It first undergoes downsampling through a linear layer, followed by the GeLU activation function, then upsampling through another linear layer, and finally, the GeLU activation function is used to restore the initial dimension. The purpose of the adapter is to allow the model to mitigate the domain differences between the training dataset and the pre-trained model dataset with the introduction of a small number of parameters, adapting to new dataset scenarios.

**Channel Modulation.** Since the feature map size extracted by ViT is  $V \in \mathbb{R}^{1024 \times 37 \times 37}$ , to match the dimensions of the feature map  $S_4$  extracted by Hiera, which is  $S_4 \in \mathbb{R}^{1152 \times 11 \times 11}$ , bilinear interpolation downsampling is first used to reduce the channel dimension to 1152. Then, depth-wise separable wavelet convolution [12] is employed to reduce both the height and width of the feature map to 11. This is implemented by the WTD module shown in Figure 3, which achieves a larger receptive field with a lower number of parameters through wavelet transformation. The RFB [13, 14] module is used to reduce the channel dimension, decreasing the number of channels in the multi-level feature maps extracted by the encoder to 64, thereby enhancing the discriminability and robustness of the feature channels.

**Feature Fusion.** We employ Content-Guided Attention [15] (CGA) to inject the semantic information of features extracted by ViT into those extracted by SAM2 Hiera. By combining spatial attention, channel attention, and pixel attention, we fuse the feature representations of the two encoders to obtain richer semantic information.

**Decoder.** To leverage high-level feature maps to guide the fusion of low-level feature maps, thereby preserving the spatial detail information of the low-level feature maps while enhancing their semantic information, thus improving the accuracy and robustness of detection results, we employ the Spatial Feature Fusion module [16] (SFF), which can dynamically adjust the weights of the output feature maps based on the correlations between feature maps of different scales. Finally, through  $1 \times 1$  point-wise convolution and bilinear interpolation upsampling, the feature maps are transformed into  $D_i \in \mathbb{R}^{1 \times 352 \times 352}$ , i.e., a single-channel image.

**Loss Function.** We employ a weighted Intersection over Union (IoU) loss and Binary Cross-Entropy (BCE) loss to measure the discrepancy between predicted and actual values [10, 13, 17], which can be expressed as:

$$\mathcal{L} = \mathcal{L}^w_{\text{IoU}} + \mathcal{L}^w_{\text{BCE}} \quad (1)$$

Additionally, we calculate such loss functions for the decoder output  $D_i$  at each level. Therefore, the overall loss function for DGSUnet is represented as:

$$\mathcal{L}_{\text{total}} = w_1 \mathcal{L}_1 + w_2 \mathcal{L}_2 + w_3 \mathcal{L}_3 \quad (2)$$

Among it,  $w_1=0.25, w_2=0.5, w_3=1$ .

## 4 Experiment

### 4.1 Datasets

To validate the performance of our model in salient object detection and camouflaged object detection, we conducted training and inference on five datasets selected from salient object detection benchmark tests and four datasets from camouflaged object detection benchmark tests.

**Salient Object Detection (SOD).** Salient Object Detection refers to enabling computer vision to mimic human vision, making it easy for attention to be drawn to prominent objects. Since its introduction in 2007, it has been widely applied in fields such as object recognition, tracking, and image segmentation. Our experiments were conducted using mainstream datasets, including DUTS [18], DUT-OMRON [19], HKU-IS [20], PASCAL-S [21], and ECSSD [22], as shown in Table 1.

**Camouflage Object Detection (COD).** Camouflage Object Detection refers to the accurate identification of camouflaged targets hidden within the surrounding environment. We selected CAMO [23], COD10K [24], CHAMELEON, and NC4K [25] for our experiments, as shown in Table 2.

### 4.2 Evaluation Metrics

To evaluate the model's prediction output results, we adhere to the requirements of salient object detection and camouflage object detection benchmarks. We utilize several metrics, including the S-measure, F-measure, E-measure, and Mean Absolute Error (MAE), to assess the accuracy of the generated prediction maps. Below, we will provide a detailed explanation of these common evaluation metrics.

**S-measure (S<sub>a</sub>)** [26]. Used to measure the structural similarity difference between the predicted map and the ground truth map, the specific formula is

$$S_a = \alpha * S_o + (1-\alpha) * S_r \quad (3)$$

where  $\alpha$  is the weight coefficient, ranging from [0,1], set to 0.5 according to benchmarking requirements,  $S_o$  represents the object-oriented structural similarity metric, and  $S_r$  represents the region-oriented structural similarity metric.

**F-measure (F<sub>B</sub>)** [27, 28]. Combining precision and recall, it is used to comprehensively evaluate model performance. The formula is expressed as:

$$F = \frac{(1+\beta^2)P \times R}{\beta^2 \times P + R} \quad (4)$$

Here,  $\beta^2$  serves as the weight to harmonize precision and recall, where  $\beta^2$  is a real number greater than 0. When  $\beta^2 < 1$ , it indicates that the evaluation places more emphasis on precision; when  $\beta^2 > 1$ , it signifies a greater emphasis on recall. P represents precision, which is the ratio of the number of correctly predicted positive samples to the total number of samples predicted as positive, while R denotes recall, which is the ratio of the number of correctly predicted positive samples to the total number of actual positive samples.

**E- measure (E<sub>φ</sub>)** [29]. It is an evaluation metric used to simulate human visual perception, based on pixel-level and image-level, to assess the local and global similarity between the predicted image and the ground truth image. The formula is defined as:

$$E_\varphi = \frac{1}{WH} \sum_{x=1}^W \sum_{y=1}^H \varphi(C(x, y) - G(x, y)) \quad (5)$$

Here,  $\varphi$  is an enhanced alignment matrix, W and H are the width and height of the input image, respectively, and  $C(x, y)$  and  $G(x, y)$  represent the pixel values at the (x, y) position in the predicted and ground truth images, respectively.

**Mean Absolute Error (M)** [30]. Measures the pixel-level accuracy difference between the predicted map and the ground truth annotation map, formulated as:

$$M = \frac{1}{WH} \sum_{x=1}^W \sum_{y=1}^H |C(x, y) - G(x, y)| \quad (6)$$

### 4.3 Train and Test

During the training phase, the input images are resized to 352×352 and 518×518 respectively for input into the Hiera and DINoV2 ViT encoders. The batch size is set to

8, and the number of training epochs is set to 50 following the benchmark testing conventions for salient object detection and camouflaged object detection. The learning rate is set to 0.001, with the optimizer chosen as AdamW [31] and a weight decay coefficient of 5e-4. Data augmentation is performed using random vertical and horizontal flips with a probability of 0.5. The code development is based on PyTorch, and the hardware resources utilized include an NVIDIA RTX4090 with 24GB of video memory. For salient object detection, 10,553 images from the DUTS dataset are used as the training set, while the remaining 5,019 images and four other datasets (DUT-OMRON, HKU-IS, PASCAL-S, and ECSSD) serve as the test set. In camouflaged object detection, 1,000 images from CAMO and 3,040 images from COD10K are used as the training set, with the remaining 250 images from CAMO, 2,026 images from COD10K, and two additional datasets (CHAMELEON and NC4K) forming the test set. In summary, both types of object detection adhere to the standard training and testing partitioning schemes of their respective benchmark tests.

During the testing phase, we normalize the output of the last decoder to the range [0,1], multiply it by 255, and convert it to an 8-bit unsigned integer type to produce the output mask grayscale image.

**Table 1.** Salient Object Detection Datasets.

Dataset name	Year	Training Set	Test Set	Description
DUTS	2017	10553	5019	The image is sourced from the ImageNet Det test set and the SUN dataset, both of which encompass a rich and diverse array of scenes and object categories.
DUT-OMRON	2013	-	5168	This dataset includes images with complex backgrounds and rich content, featuring one or more prominent objects in each image.
HKU-IS	2015	-	4447	The dataset includes a large number of images featuring multiple salient objects captured in complex scenes, covering various spatial distributions where objects exhibit both connected and disconnected relationships.
PASCAL-S	2014	-	850	The annotation of this dataset primarily relies on human eye fixation points, hence its difficulty is relatively high.
ECSSD	2013	-	1000	The ECSSD dataset is an extension of the CSSD dataset, with each image containing relatively complex backgrounds and structured information.

**Table 2.** Camouflage Object Detection Datasets.

Dataset name	Year	Training Set	Test Set	Description
CAMO	2019	1000	250	The dataset covers natural camouflage (such as camouflaged animals) and artificial camouflage (such as body paint and military camouflage), presenting challenges in recognition
COD10K	2020	3040	2026	The dataset's camouflage target categories include terrestrial organisms, marine organisms, flying organisms, and amphibians under natural camouflage, with targets sized into three levels: large, medium, and small. This is currently the largest camouflage target dataset available.
CHAMELEON	2018	-	76	This is an un-peer-reviewed public dataset containing 76 images collected from the internet using the keyword 'camouflaged animals'. This is currently the largest camouflage target
NC4K	2021	-	4121	test set, with the majority of the targets featuring natural camouflage, along with a small number of artificially camouflaged ones.

#### 4.4 Result

The DGSUnet model achieves state-of-the-art performance in benchmark tests for salient object detection and camouflaged object detection, essentially surpassing or matching the current SOTA (State-of-the-Art) methods.

The benchmark test results for salient object detection are shown in Table 3, where DGSUnet slightly outperforms SAM2-Unet across five datasets. In the benchmark test results for camouflaged object detection, as shown in Table 4, DGSUnet generally performs better than SAM2-Unet in four datasets, with performance improvements exceeding those observed in the salient object benchmark tests.

Our method is compared with the latest SOTA method, SAM2-Unet, in both salient object detection and camouflaged object detection, with visual comparison results presented in Figures 4 and 5, respectively. Clearly, our method excels in salient object detection, effectively suppressing interfering objects in the image and accurately outputting the main object mask. In camouflaged object detection, compared to SAM2-Unet, the segmentation performance is significantly better, particularly in scenarios with subtle background differences and small object segmentation.

#### 4.5 Ablation Study

To verify the effectiveness of the features extracted by the DINOv2 ViT feature extractor when injected into the last layer feature map extracted by the SAM2 Hiera backbone network, and to demonstrate its role in guiding the multi-scale feature collaboration and fusion of SAM2, this paper conducts ablation experiments, with the results presented in Table 5.

**Table 3.** Performance Results of Salient Object Detection Benchmark Tests.

Methods	DUTS-TE			DUT-OMRON			HKU-IS			PASCAL-S			ECSSD		
	S <sub>α</sub>	E <sub>φ</sub>	M												
U2Net[32]	0.874	0.884	0.044	0.847	0.872	0.054	0.916	0.948	0.031	0.844	0.850	0.074	0.928	0.925	0.033
ICON[33]	0.889	0.914	0.037	0.845	0.879	0.057	0.920	0.959	0.029	0.861	0.893	0.064	0.929	0.954	0.032
EDN[34]	0.892	0.925	0.035	0.850	0.877	0.049	0.924	0.955	0.026	0.865	0.902	0.062	0.927	0.951	0.032
MENet[35]	0.905	0.937	0.028	0.850	0.891	0.045	0.927	0.966	0.023	0.872	0.913	0.054	0.928	0.954	0.031
SAM2-Unet[10]	0.934	0.959	0.020	0.884	0.912	0.039	0.941	<b>0.971</b>	0.019	0.894	0.931	0.043	0.950	0.970	0.020
DGSUnet(Ours)	<b>0.934</b>	<b>0.959</b>	<b>0.020</b>	<b>0.885</b>	<b>0.915</b>	<b>0.039</b>	<b>0.945</b>	0.969	<b>0.019</b>	<b>0.898</b>	<b>0.935</b>	<b>0.042</b>	<b>0.953</b>	<b>0.972</b>	<b>0.018</b>

**Table 4.** Performance Results of Camouflaged Object Detection Benchmark Tests.

Methods	CHAMELEON				CAMO				COD10K				NC4K			
	S <sub>α</sub>	F <sub>β</sub>	E <sub>φ</sub>	M	S <sub>α</sub>	F <sub>β</sub>	E <sub>φ</sub>	M	S <sub>α</sub>	F <sub>β</sub>	E <sub>φ</sub>	M	S <sub>α</sub>	F <sub>β</sub>	E <sub>φ</sub>	M
SINet[24]	0.872	0.832	0.936	0.034	0.745	0.712	0.804	0.092	0.776	0.667	0.864	0.043	0.808	0.768	0.871	0.058
PFNet[36]	0.882	0.820	0.931	0.033	0.782	0.751	0.841	0.085	0.800	0.676	0.877	0.040	0.829	0.779	0.887	0.053
ZoomNet[37]	0.902	0.858	0.943	0.024	0.820	0.792	0.877	0.066	0.838	0.740	0.888	0.029	0.853	0.814	0.896	0.043
FEDER[38]	0.903	0.856	0.947	0.026	0.836	0.807	0.897	0.066	0.844	0.784	0.911	0.029	0.862	0.824	0.913	0.042
SAM2-Unet[10]	0.914	0.863	<b>0.961</b>	0.022	0.884	<b>0.861</b>	<b>0.932</b>	0.042	0.880	0.789	0.936	0.021	0.901	0.863	0.941	0.029
DGSUnet(Ours)	<b>0.923</b>	<b>0.869</b>	0.955	<b>0.020</b>	<b>0.889</b>	0.855	0.931	<b>0.041</b>	<b>0.891</b>	<b>0.819</b>	<b>0.947</b>	<b>0.019</b>	<b>0.909</b>	<b>0.868</b>	<b>0.948</b>	<b>0.026</b>

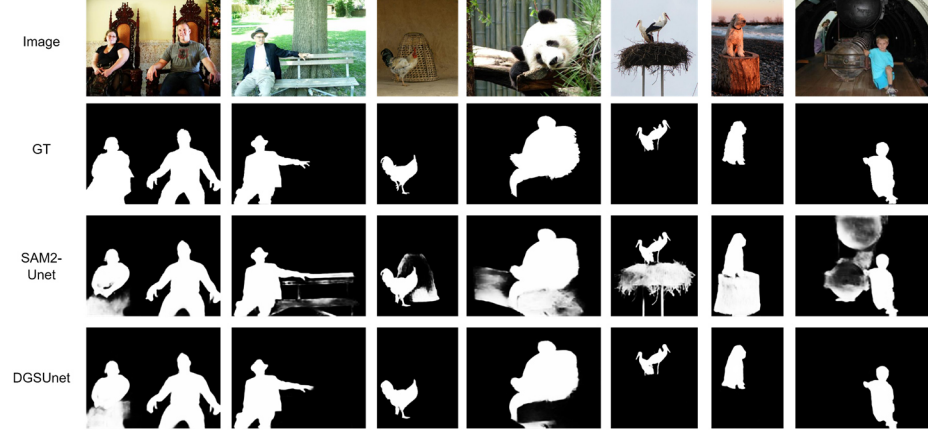


**Fig. 4.** Camouflaged Object Detection Visualization Results.



**Fig. 5.** Salient Object Detection Visualization Results.

**Table 5.** Ablation Study Result.

Methods	DUTS-TE			DUT-OMRON			CAMO			COD10K				
	$S_\alpha$	$E_\phi$	M	$S_\alpha$	$E_\phi$	M	$S_\alpha$	$F_\beta$	$E_\phi$	M	$S_\alpha$	$F_\beta$	$E_\phi$	M
A	0.931	0.955	0.023	0.880	0.909	0.041	0.881	0.852	0.924	0.045	0.879	0.800	0.938	0.020
B	0.926	0.950	0.025	0.879	0.907	0.044	0.875	0.848	0.919	0.048	0.868	0.792	0.933	0.022
C	0.928	0.952	0.024	0.880	0.907	0.042	0.880	0.851	0.922	0.043	0.881	0.801	0.939	0.020
DGSUnet(Ours)	<b>0.934</b>	<b>0.959</b>	<b>0.020</b>	<b>0.885</b>	<b>0.915</b>	<b>0.039</b>	<b>0.889</b>	<b>0.855</b>	<b>0.931</b>	<b>0.041</b>	<b>0.891</b>	<b>0.819</b>	<b>0.947</b>	<b>0.019</b>

In this, A represents DGSUnet with the DINOv2 ViT feature extraction module removed; B indicates that in DGSUnet, the DINOv2 ViT does not use the output feature map of the last layer, but instead extracts the output feature maps from its four different

hierarchical Block blocks, which are respectively injected into the four feature maps of SAM2 Hiera; C signifies that the output feature map of the last layer of DINOv2 ViT in DGSUnet is injected into the four feature maps of SAM2 Hiera.

Clearly, the fusion of features extracted solely from the last layer of DINOv2 ViT with the feature map from the last layer of SAM2 Hiera proves to be the most effective.

## 5 Conclusion

In this paper, we propose an improved model DGSUnet based on the Unet network structure, which utilizes features extracted by DINOv2 to guide the multi-scale feature synergy of SAM2. This model achieves state-of-the-art performance in benchmark tests for salient object detection and camouflaged object detection, and can be widely applied to general image segmentation. The innovative integration of SAM2 and DINOv2's image encoding capabilities is demonstrated through ablation experiments, proving that our method maximizes the retention of the model's global perception and local capture abilities, achieving superior performance beyond that of a single encoder.

## References

1. Kirillov, A., Mintun, E., Ravi, N., Mao, H., Rolland, C., Gustafson, L., Xiao, T., Whitehead, S., Berg, A., Lo, W.-Y., Dollár, P., Girshick, R.B.: Segment Anything. 2023 IEEE/CVF International Conference on Computer Vision (ICCV) 3992-4003 (2023)
2. Oquab, M., Dariseti, T., Moutakanni, T., Vo, H., Szafraniec, M., Khalidov, V., Fernandez, P., Haziza, D., Massa, F., El-Nouby, A., Assran, M., Ballas, N., Galuba, W., Howes, R., Huang, P.-Y., Li, S.-W., Misra, I., Rabbat, M., Sharma, V., Synnaeve, G., Xu, H., Jegou, H., Mairal, J., Labatut, P., Joulin, A., Bojanowski, P.: DINOv2: Learning Robust Visual Features without Supervision. arXiv.org (2023)
3. Ronneberger, O., Fischer, P., Brox, T.: U-Net: Convolutional Networks for Biomedical Image Segmentation. Medical Image Computing and Computer-Assisted Intervention – MICCAI 2015 abs/1505.04597, 234-241 (2015)
4. Zhou, Z., Siddiquee, M.R., Tajbakhsh, N., Liang, J.: UNet++: A Nested U-Net Architecture for Medical Image Segmentation. Deep Learning in Medical Image Analysis and Multi-modal Learning for Clinical Decision Support 11045, 3-11 (2018)
5. Jha, D., Smedsrød, P.H., Riegler, M.A., Johansen, D., Lange, T.D., Halvorsen, P., D. Johansen, H.: ResUNet++: An Advanced Architecture for Medical Image Segmentation. In: 2019 IEEE International Symposium on Multimedia (ISM), pp. 225-2255. IEEE, (Year)
6. Chen, J., Mei, J., Li, X., Lu, Y., Yu, Q., Wei, Q., Luo, X., Xie, Y., Adeli, E., Wang, Y., Lungren, M., Zhang, S., Xing, L., Lu, L., Yuille, A.L., Zhou, Y.: TransUNet: Rethinking the U-Net architecture design for medical image segmentation through the lens of transformers. Med. Image Anal. 97, 103280 (2024)
7. Cao, H., Wang, Y., Chen, J., Jiang, D., Zhang, X., Tian, Q., Wang, M.: Swin-Unet: Unet-like Pure Transformer for Medical Image Segmentation. Computer Vision – ECCV 2022 Workshops 205-218 (2021)

8. Liu, Z., Lin, Y., Cao, Y., Hu, H., Wei, Y., Zhang, Z., Lin, S., Guo, B.: Swin Transformer: Hierarchical Vision Transformer using Shifted Windows. 2021 IEEE/CVF International Conference on Computer Vision (ICCV) 9992-10002 (2021)
9. Chen, T., Zhu, L., Ding, C., Cao, R., Wang, Y., Zhang, S., Li, Z., Sun, L., Zang, Y.-D., Mao, P.: SAM-Adapter: Adapting Segment Anything in Underperformed Scenes. 2023 IEEE/CVF International Conference on Computer Vision Workshops (ICCVW) 3359-3367 (2023)
10. Xiong, X., Wu, Z., Tan, S., Li, W., Tang, F., Chen, Y., Li, S., Ma, J., Li, G.: SAM2-UNet: Segment Anything 2 Makes Strong Encoder for Natural and Medical Image Segmentation. arXiv.org (2024)
11. Caron, M., Touvron, H., Misra, I., Jegou, H., Mairal, J., Bojanowski, P., Joulin, A.: Emerging Properties in Self-Supervised Vision Transformers. In: 2021 IEEE/CVF International Conference on Computer Vision (ICCV), pp. 9630-9640. IEEE, (Year)
12. Finder, S.E., Amoyal, R., Treister, E., Freifeld, O.: Wavelet Convolutions for Large Receptive Fields. Computer Vision – ECCV 2024, pp. 363-380. Springer Nature Switzerland, Cham (2024)
13. Fan, D.-P., Ji, G.-P., Zhou, T., Chen, G., Fu, H., Shen, J., Shao, L.: PraNet: Parallel Reverse Attention Network for Polyp Segmentation. Medical Image Computing and Computer Assisted Intervention – MICCAI 2020, vol. abs/2006.11392, pp. 263-273. Springer International Publishing, Cham (2020)
14. Liu, S., Huang, D., Wang, Y.: Receptive Field Block Net for Accurate and Fast Object Detection. Computer Vision – ECCV 2018 abs/1711.07767, 404-419 (2017)
15. Chen, Z., He, Z., Lu, Z.-m.: DEA-Net: Single Image Dehazing Based on Detail-Enhanced Convolution and Content-Guided Attention. IEEE Trans. Image Process. 33, 1002-1015 (2023)
16. Ma, X., Yang, J., Hong, T., Ma, M., Zhao, Z., Feng, T., Zhang, W.: STNet: Spatial and Temporal feature fusion network for change detection in remote sensing images. In: 2023 IEEE International Conference on Multimedia and Expo (ICME), pp. 2195-2200. IEEE, (Year)
17. Wei, J., Wang, S., Huang, Q.: F3Net: Fusion, Feedback and Focus for Salient Object Detection. Proceedings of the AAAI Conference on Artificial Intelligence 34, 12321-12328 (2019)
18. Wang, L., Lu, H., Wang, Y., Feng, M., Wang, D., Yin, B., Ruan, X.: Learning to Detect Salient Objects with Image-Level Supervision. 2017 IEEE Conference on Computer Vision and Pattern Recognition (CVPR) 3796-3805 (2017)
19. Yang, C., Zhang, L., Lu, H., Ruan, X., Yang, M.-H.: Saliency Detection via Graph-Based Manifold Ranking. In: 2013 IEEE Conference on Computer Vision and Pattern Recognition, pp. 3166-3173. IEEE, (Year)
20. Li, G., Yu, Y.: Visual saliency based on multiscale deep features. 2015 IEEE Conference on Computer Vision and Pattern Recognition (CVPR) 5455-5463 (2015)
21. Li, Y., Hou, X., Koch, C., Rehg, J.M., Yuille, A.L.: The Secrets of Salient Object Segmentation. In: 2014 IEEE Conference on Computer Vision and Pattern Recognition, pp. 280-287. IEEE, (Year)
22. Yan, Q., Xu, L., Shi, J., Jia, J.: Hierarchical Saliency Detection. 2013 IEEE Conference on Computer Vision and Pattern Recognition 1155-1162 (2013)
23. Le, T.-N., Nguyen, T.V., Nie, Z., Tran, M.-T., Sugimoto, A.: Anabanch network for camouflaged object segmentation. Comput. Vision Image Understanding 184, 45-56 (2019)

24. Fan, D.-P., Ji, G.-P., Sun, G., Cheng, M.-M., Shen, J., Shao, L.: Camouflaged Object Detection. 2020 IEEE/CVF Conference on Computer Vision and Pattern Recognition (CVPR) 2774-2784 (2020)
25. Lyu, Y., Zhang, J., Dai, Y., Li, A., Liu, B., Barnes, N., Fan, D.-P.: Simultaneously Localize, Segment and Rank the Camouflaged Objects. 2021 IEEE/CVF Conference on Computer Vision and Pattern Recognition (CVPR) 11586-11596 (2021)
26. Fan, D.-P., Cheng, M.-M., Liu, Y., Li, T., Borji, A.: Structure-Measure: A New Way to Evaluate Foreground Maps. In: 2017 IEEE International Conference on Computer Vision (ICCV), pp. 4558-4567. IEEE, (Year)
27. Achanta, R., Hemami, S., Estrada, F., Süsstrunk, S.: Frequency-tuned salient region detection. 2009 IEEE Conference on Computer Vision and Pattern Recognition 1597-1604 (2009)
28. Margolin, R., Zelnik-Manor, L., Tal, A.: How to Evaluate Foreground Maps. 2014 IEEE Conference on Computer Vision and Pattern Recognition 248-255 (2014)
29. Fan, D.-P., Gong, C., Cao, Y., Ren, B., Cheng, M.-M., Borji, A.: Enhanced-alignment Measure for Binary Foreground Map Evaluation. Proceedings of the Twenty-Seventh International Joint Conference on Artificial Intelligence 698-704 (2018)
30. Perazzi, F., Krähenbühl, P., Pritch, Y., Sorkine-Hornung, A.: Saliency filters: Contrast based filtering for salient region detection. 2012 IEEE Conference on Computer Vision and Pattern Recognition 733-740 (2012)
31. Loshchilov, I., Hutter, F.: Decoupled Weight Decay Regularization. In: International Conference on Learning Representations. (Year)
32. Qin, X., Zhang, Z., Huang, C., Dehghan, M., Zaiane, O.R., Jägersand, M.: U2-Net: Going Deeper with Nested U-Structure for Salient Object Detection. Pattern Recognit. 106, 107404 (2020)
33. Zhuge, M., Fan, D.-P., Liu, N., Zhang, D., Xu, D., Shao, L.: Salient Object Detection via Integrity Learning. IEEE Trans. Pattern Anal. Mach. Intell. 45, 3738-3752 (2021)
34. Wu, Y.-H., Liu, Y., Zhang, L., Cheng, M.-M.: EDN: Salient Object Detection via Extremely-Downsampled Network. IEEE Trans. Image Process. 31, 3125-3136 (2020)
35. Wang, Y., Wang, R., Fan, X., Wang, T., He, X.: Pixels, Regions, and Objects: Multiple Enhancement for Salient Object Detection. In: 2023 IEEE/CVF Conference on Computer Vision and Pattern Recognition (CVPR), pp. 10031-10040. IEEE, (Year)
36. Mei, H., Ji, G.-P., Wei, Z., Yang, X., Wei, X., Fan, D.-P.: Camouflaged Object Segmentation with Distraction Mining. 2021 IEEE/CVF Conference on Computer Vision and Pattern Recognition (CVPR) 8768-8777 (2021)
37. Pang, Y., Zhao, X., Xiang, T.-Z., Lihe, Z., Lu, H.: Zoom In and Out: A Mixed-scale Triplet Network for Camouflaged Object Detection. 2022 IEEE/CVF Conference on Computer Vision and Pattern Recognition (CVPR) 2150-2160 (2022)
38. He, C., Li, K., Zhang, Y., Tang, L., Zhang, Y., Guo, Z., Li, X.: Camouflaged Object Detection with Feature Decomposition and Edge Reconstruction. 2023 IEEE/CVF Conference on Computer Vision and Pattern Recognition (CVPR) 22046-22055 (2023)